

Formation of Thiolate and Phosphonate Adlayers on Indium–Tin Oxide: Optical and Electronic Characterization

Scott H. Brewer, Derek A. Brown, and Stefan Franzen*

Department of Chemistry, North Carolina State University, Raleigh, North Carolina 27695

Received December 10, 2001. In Final Form: May 15, 2002

Variable angle reflectance Fourier transform infrared spectroscopy and X-ray photoelectron spectroscopy were used to investigate adlayers on indium–tin oxide (ITO) and fluorine-doped tin oxide surfaces. A close-packed, ordered adlayer was observed to form on both surfaces by 1-hexadecanethiol through thiolate–indium or thiolate–tin bonding on the two surfaces, respectively. Additionally, a close-packed, ordered adlayer of 12-phosphonododecanoic acid was observed to form on ITO through a phosphonate–indium bonding interaction. The chain length dependence of adlayer formation was studied using alkane thiols of varying chain lengths, and the enthalpic factors affecting adlayer formation were modeled using density functional theory calculations along with periodic boundary conditions.

Introduction

Thin organic films on gold have shown tremendous utility for surface attachment strategies.^{1–8} Recently, there has been a great deal of interest in expanding the repertoire of substrates for thin film formation to include metal oxides and selenides.^{3,9–15} These materials offer a range of new physical properties that are important for the design of new spectroscopic and electrochemical applications.^{16–20} The goals of such studies include the fundamental characterization of the films themselves but may also be key to development of new evanescent wave spectroscopies.¹³ The stability of self-assembled monolayers is determined by both the bonding interaction with the metal or metal chalcogenide substrate and the hydrophobic effect between aliphatic regions of adlayer molecules. The determination of the relative strength of

these competing factors on gold has been well studied, particularly in the case of the family of derivatized alkane thiols.^{3,21}

Because thiols have been widely used for the creation of self-assembled monolayers, it is logical to consider their application on metal chalcogenides. Although the interaction of thiols with metal oxides is not necessarily as strong as that with gold,¹⁵ thiols may still form adlayers on metal oxide surfaces under certain deposition conditions. The nature of the bonding of thiols to indium–tin oxide (ITO) surfaces has recently been characterized as a bonding interaction between thiolate and indium.²² A recent study has also indicated that thiols can form adlayers on zinc selenide.¹³ Previous work has showed the formation of adlayers of phosphonic and carboxylic acids on ITO.¹⁵ However, here we compare the relative affinities of these two functional groups for ITO. In this study, we compare thiols (or thiolates) with phosphonates and sulfonates on indium–tin oxide and fluorine-doped tin oxide (SFO) surfaces. While thiols and phosphonates form stable surface layers for alkane chain lengths of greater than 16 and 12, respectively, sulfonates do not form stable adlayers. Phosphonic acid functional groups were found to preferentially interact with the ITO surface relative to carboxylic acid functional groups. We show that variable angle reflectance Fourier transform infrared (FTIR) spectroscopy and X-ray photoelectron spectroscopy (XPS) are powerful tools for examination of the organization of surface layers including their order and relative surface coverage. A novel application of density functional theory (DFT) is presented using periodic boundary conditions to address the relative strength of chemical bonding between metal atoms and thiolate or phosphonate layers compared to nonbonding interactions between aliphatic chains. Although solvent is not explicitly included, these studies indicate the relative importance of hydrophobic interactions in stabilizing films. Both DFT calculations and experimental observations such as the presence of phosphonate layers and absence of sulfonate layers indicate that there is indeed a strong ionic bonding interaction

* To whom correspondence should be addressed. Phone: (919)-515-8915. Fax: (919)-515-8909.

- (1) Terril, R.; Tanzer, T.; Bohn, P. *Langmuir* **1998**, *14*, 845–854.
- (2) Bain, C.; Biebuyck, H.; Whitesides, G. *Langmuir* **1989**, *5*, 723–727.
- (3) Ulman, A. *Chem. Rev.* **1996**, *96*, 1533–1554.
- (4) Karyakin, A.; Presnova, G.; Rubtsova, M.; Egorov, A. *Anal. Chem.* **2000**, *72*, 3805–3811.
- (5) Kitano, H.; Taira, Y.; Yamamoto, H. *Anal. Chem.* **2000**, *72*, 2976–2980.
- (6) Kittredge, K.; Fox, M.; Whitesell, J. *J. Phys. Chem. B* **2001**, *105*, 10594–10599.
- (7) Ringsdorf, H. *Macromolecules* **1997**, *30*, 5913–5919.
- (8) Nakashima, N. *Langmuir* **1999**, *15*, 3823–3830.
- (9) Tamada, M.; Koshikawa, H.; Hosoi, F.; Suwa, T. *Thin Solid Films* **1998**, *315*, 40–43.
- (10) Folkers, J.; Gorman, C.; Laibinis, P.; Buchholz, S.; Whitesides, G. *Langmuir* **1995**, *11*, 813–824.
- (11) Allara, D.; Nuzzo, R. *Langmuir* **1985**, *1*, 45–52.
- (12) Allara, D.; Nuzzo, R. *Langmuir* **1985**, *1*, 52–66.
- (13) Noble-Luginbuhl, A.; Nuzzo, R. *Langmuir* **2001**, *17*, 3937–3944.
- (14) Purvis, K.; Lu, G.; Schwartz, J.; Bernasek, S. *J. Am. Chem. Soc.* **2000**, *122*, 1808–1809.
- (15) Gardner, T.; Frisbie, C.; Wrighton, M. *J. Am. Chem. Soc.* **1995**, *117*, 6927–6933.
- (16) VanderKam, S.; Gawalt, E.; Schwartz, J.; Bocarsly, A. *Langmuir* **1999**, *15*, 6598–6600.
- (17) Armistead, P.; Thorp, H. *Anal. Chem.* **2000**, *72*, 3764–3770.
- (18) Zotti, G.; Schiavon, G.; Zecchin, S.; Berlin, A.; Pagani, G. *Langmuir* **1998**, *14*, 1728–1733.
- (19) Li, L.; Wang, R.; Fitzsimmons, M.; Li, D. *J. Phys. Chem. B* **2000**, *104*, 11195–11201.
- (20) Oh, S.; Yun, Y.; Kim, D.; Han, S. *Langmuir* **1999**, *15*, 4690–4692.

(21) Lavrich, D.; Wetterer, S.; Bernasek, S.; Scoles, G. *J. Phys. Chem. B* **1998**, *102*, 3456–3465.

(22) Yan, C.; Zharnikov, M.; Golzhauser, A.; Grunze, M. *Langmuir* **2000**, *16*, 6208–6215.

between the adlayer molecules and metal atoms in the metal oxide substrate.

Methods and Materials

Chemicals and Substrates. 1-Hexadecanethiol, dodecanethiol, octanethiol, and dimethyl sulfoxide (DMSO) were used as received from Sigma-Aldrich. Sodium dodecyl sulfate (SDS) was used as received from Bio-Rad Laboratories. 12-Phosphonododecanoic acid was obtained from Xantho, Inc. Millipore 18 M Ω cm deionized water (Barnstead E-Pure) was used for aqueous solutions. ITO electrodes were received from Delta Technologies, Ltd., and were comprised of 90% indium oxide and 10% tin oxide. The ITO electrodes had a nominal thickness of 1500 Å and a sheet resistance of 8–12 Ω/\square . The substrate for the ITO electrodes was polished float (soda-lime) glass. The SFO electrodes were obtained from PPG Industries, Inc., and had a sheet resistance of 49–51 Ω/\square , while the gold electrodes were obtained from Evaporated Films, Inc.

Deposition on ITO and SFO Electrodes. The ITO and SFO electrodes were cleaned via 20 min of UV/O₃ (UVO cleaner (UVO-60), model number 42, Jelight Co., Inc.) to yield a clean hydrophilic surface.²² Contact angle measurements (NRL C. A. goniometer, model 100-00, Rame-Hart Inc.) determined that the surface was hydrophilic after cleaning. The sheet resistances of these electrodes were measured with a four-point probe consisting of a Signatone D27M probe station, a Keithley 224 programmable current source, and a Hewlett-Packard 3456A digital voltmeter. The clean electrodes were then immersed for 16 h in one of the deposition solutions. The deposition solutions were 10 mM 12-phosphonododecanoic acid in DMSO or 50/50 (v/v) DMSO/18 M Ω cm H₂O, 10 mM SDS in 18 M Ω cm H₂O or 50/50 (v/v) DMSO/18 M Ω cm H₂O, neat 1-hexadecanethiol, neat dodecanethiol, and neat octanethiol. Then electrodes immersed in either 12-phosphonododecanoic acid or SDS were rinsed with 18 M Ω cm H₂O followed by drying the electrodes with N₂ gas. The electrodes immersed in 1-hexadecanethiol, dodecanethiol, or octanethiol were rinsed with ethanol and dried with N₂ gas. Then the electrodes first immersed in neat 1-hexadecanethiol (16 h) were then immersed in 10 mM 12-phosphonododecanoic acid in 50/50 (v/v) DMSO/18 M Ω cm H₂O (16 h), rinsed with 18 M Ω cm H₂O, and dried with N₂ gas. Also, the electrodes first immersed in 10 mM 12-phosphonododecanoic acid in 50/50 (v/v) DMSO/18 M Ω cm H₂O (16 h) were then immersed in 1-hexadecanethiol (16 h), rinsed with ethanol, and dried with N₂ gas.

Reflectance FTIR Spectroscopy. The variable angle reflectance FTIR spectra were recorded using a Spectra-Tech variable angle reflectance attachment (The Veemax) in a Nicolet 550 Magna-IR spectrometer. The angle of incidence ranged from 40 to 70°. An infrared polarizer was used to obtain s- (horizontal) or p- (vertically) polarized light. A ratio of the single beam spectra of bare ITO electrodes, SFO electrodes, or glass to a single beam spectrum of a gold electrode was performed to obtain the reflection spectrum of the ITO, SFO, or glass. The spectra of the material deposited on the electrodes were obtained by taking a ratio of the single beam spectra of the deposited material on the electrode to one of the bare electrode. The rotational lines from gaseous water were subtracted from these spectra. The solid and solution FTIR spectra of the compounds were taken using an IR microscope (model number UMA-500) attached to a Bio-Rad Digilab FTS 6000 FTIR spectrometer equipped with a Cassegrainian objective containing a germanium crystal for single pass attenuated total reflection (ATR). Both FTIR spectrometers were equipped with a liquid nitrogen cooled MCT/A detector and were recorded at a resolution of 4 cm⁻¹ with a spectral range of 650–4000 cm⁻¹. All IR spectra were the result of the average of 256 scans and were recorded at room temperature. FTIR studies of UV/O₃-cleaned ITO slides showed the presence of little or no adventitious hydrocarbon contamination. ITO slides as received from Delta Technologies, Ltd., have a substantial hydrocarbon surface contamination.

X-ray Photoelectron Spectroscopy. XPS spectra were recorded on a Riber LAS 2000 surface analysis system equipped with a cylindrical mirror analyzer (CMA) and a MAC2 analyzer with Mg K α X-rays (model CX 700 (Riber source)) ($h\nu$ = 1253.6 eV). The elemental scans had a resolution of 1.0 eV and were the

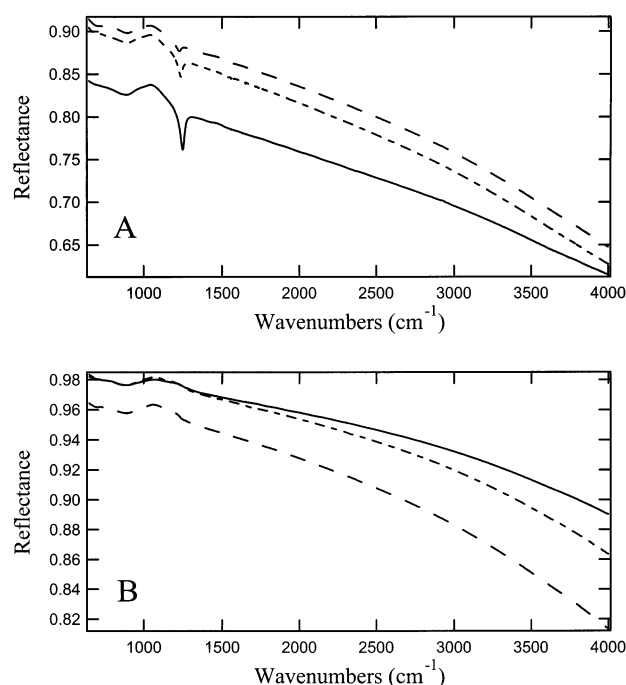


Figure 1. Variable angle reflectance FTIR spectra obtained from a ratio of an ITO electrode to gold. Spectra shown are for angles of incidence of 50° (---), 60° (-.-), and 70° (solid line) for p-polarized (A) and s-polarized (B) IR light.

result of either 5 or 20 scans (all spectra were normalized to 5 scans). XPS spectra were smoothed using a 9 point (second-order) Savitzky-Golay algorithm and baseline corrected, and the peaks were fitted using Gaussian/Lorentzian (90/10) line shapes. The phosphorus and sulfur 2p 3/2 and 1/2 angular momentum components were fitted with a fixed 2:1 peak area ratio.

Density Functional Theory Calculations. The geometry optimization, single point energy, and vibrational frequency calculations of the molecules were done using the MSI (Molecular Simulations, Inc.) quantum chemistry software program DMol3 at the North Carolina Supercomputer Center (NCSC) on either the SGI Origin 2400 or the IBM RS/6000 SP. DMol3 is an ab initio (first principles) software package that utilizes density functional theory.²³ These calculations were done in the gas phase or with periodic boundary conditions using the DNP basis set, the GGA functional, and the method of finite differences for calculating the vibrational frequencies. The MSI software Insight II was used to build the models and to visualize the eigenvector projections of the vibrational modes of the molecules. The intensities of the normal modes calculated in the gas phase were used for the corresponding normal modes in the periodic boundary condition calculations.

Results

Reflectance FTIR Spectra of ITO. ITO films have sufficiently high reflectivity in the infrared region to permit the acquisition of reflectance FTIR spectra of adlayers on ITO in a grazing-angle geometry. Parts A and B of Figure 1 show the variable angle reflectance FTIR spectra of an ITO electrode for angles of incidence from 50 to 70° for p- and s-polarized light, respectively. There are several features of these spectra that are important for consideration in optical detection of adlayer formation such as the relatively high reflectance of ITO in the mid-IR. In the methylene (CH₂) stretching region near 3000 cm⁻¹, the reflectance is >0.7 for ITO for p-polarized light (usually employed in studies on metallic surfaces due to surface selection rules)²⁴ in the grazing-angle geometry. The

(23) Delley, B. *J. Chem. Phys.* **1990**, *92*, 508–517.

(24) Parikh, A.; Allara, D. *J. Chem. Phys.* **1992**, *96*, 927–944.

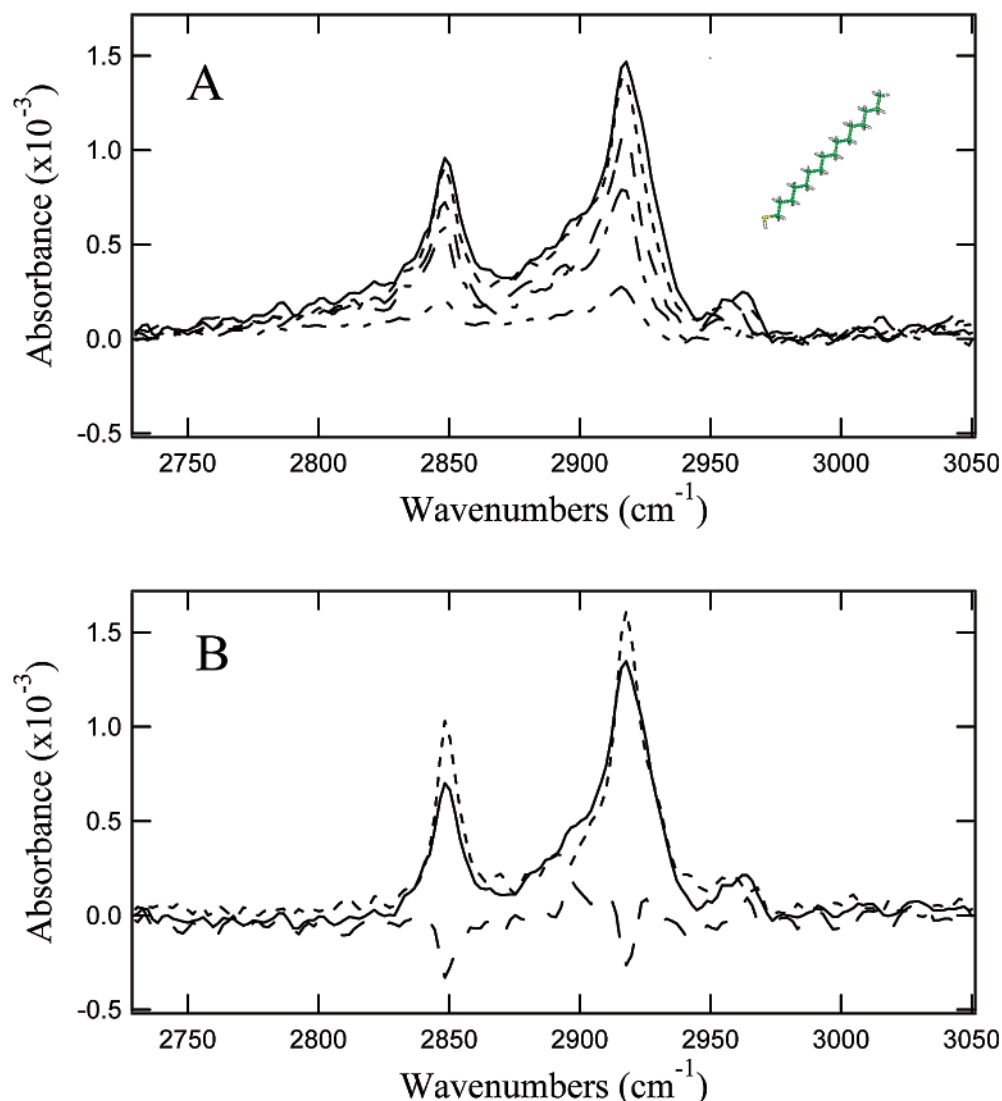


Figure 2. (A) Baseline-corrected variable angle reflectance FTIR spectra obtained from a ratio of 1-hexadecanethiol on ITO to bare ITO. The spectra shown are for angles of incidence of 40° (---), 50° (-.-), 60° (···), and 70° (solid line) for p-polarized IR light and 70° for s-polarized light (- - -). (Inset: model of 1-hexadecanethiol). (B) Baseline-corrected reflectance FTIR spectra (incidence angle of 70° with p-polarized radiation) obtained from a ratio of 1-hexadecanethiol on ITO to bare ITO (solid line), a ratio of 1-hexadecanethiol on SFO to bare SFO (- - -), and the subtraction of the spectrum of 1-hexadecanethiol on ITO from the spectrum of 1-hexadecanethiol on SFO (-.-). The bare (reference) substrate was cleaned via 20 min of UV/O₃, while the monolayer deposition occurred for 16 h.

reflectance for both p- and s-polarized spectra decreases in the wavenumber range from 1500 to 4000 cm⁻¹ due to the onset of the plasmon absorption of ITO as discussed elsewhere.²⁵ The reflectance for the p-polarized spectra increases with decreasing angle of incidence while the opposite is true for s-polarized light, thus suggesting that an angle of 50–70° is optimal for detection of surface adlayers. The longitudinal optical (LO) and transverse optical (TO) Si–O–Si stretching modes are observed at 1248 and 1064 cm⁻¹, respectively, for an incident angle of 70° and p-polarized radiation. The correlation of the intensity of this band to the skin depth of the ITO film is considered elsewhere.²⁵ In this study, it is important to note that interference from these glass bands can complicate the analysis of any features from surface adlayers that may fall in the region from 900 to 1300 cm⁻¹. Fortunately, the most important features occur elsewhere and are easily distinguished from the glass bands.

Deposition of Alkane Thiols, Phosphonates, and Sulfonates. *FTIR Characterization.* Figure 2A shows the variable angle reflectance FTIR spectra of a 1-hexadecanethiol adlayer on an ITO electrode. The figure shows

spectra corresponding to angles of incidence of 40, 50, 60, and 70° for p-polarized infrared light and the spectrum of s-polarized light at an incident angle of 70°. The intensities of the bands corresponding to the symmetric and asymmetric stretches of the CH₂ groups and asymmetric CH₃ stretches decrease as the incident angle for the p-polarized spectra decreases. The observed peaks for the s-polarized spectrum at 70° of incidence are significantly less intense as compared to those of the p-polarized spectra at the same angle of incidence. Figure 2B shows the reflectance FTIR spectra of an adlayer of 1-hexadecanethiol on either an ITO or SFO electrode corresponding to an angle of incidence of 70° and p-polarized light. The figure also shows the subtraction of these two spectra illustrating that the peak widths (of the previously mentioned vibrations) are the same for the monolayer on both electrodes but the intensity of the signal is greater on SFO. Table 1 gives the values of the various vibrational frequencies on these two metal oxide surfaces and for neat 1-hexadecanethiol.

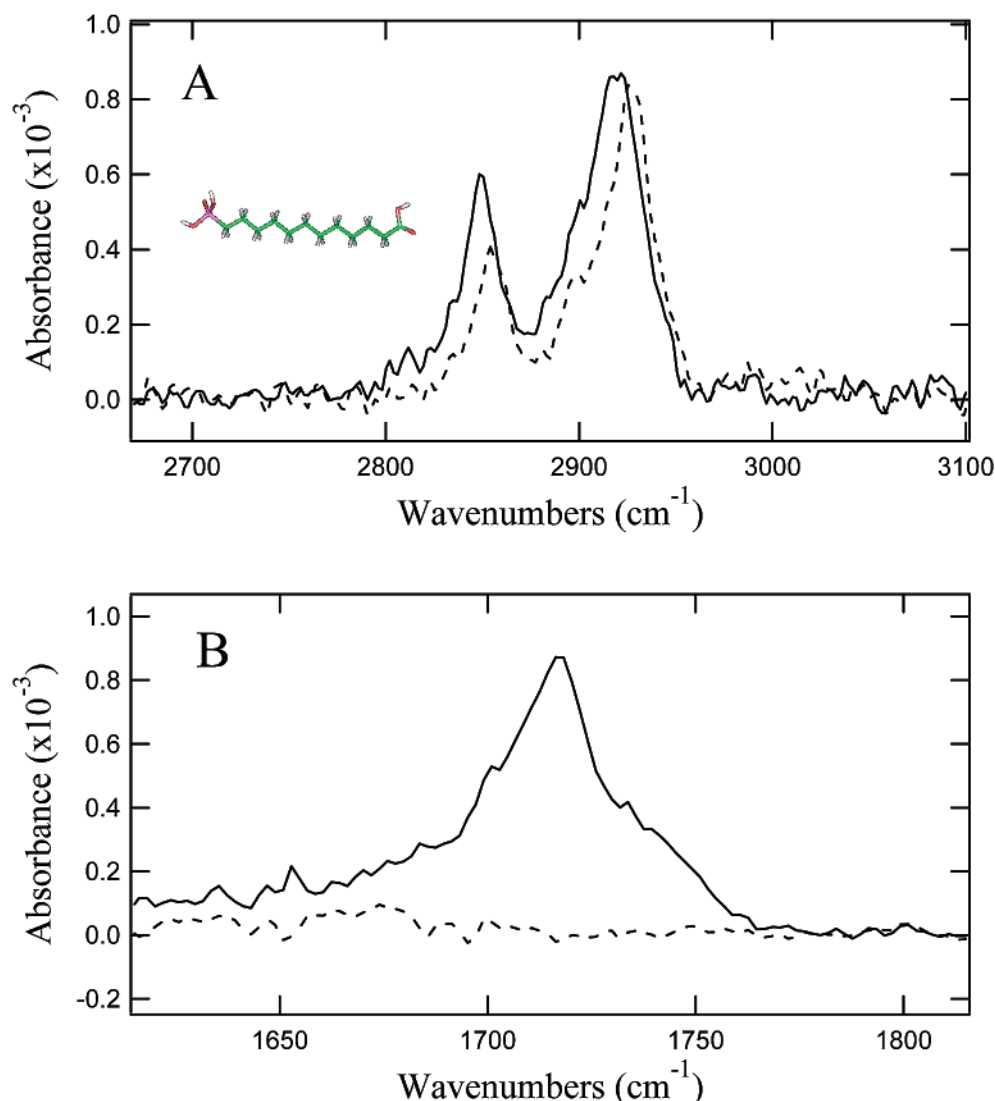


Figure 3. Baseline-corrected reflectance FTIR spectra obtained from a ratio of 12-phosphonododecanoic acid (deposited from 50/50 (v/v) DMSO/18 MΩ cm H₂O (solid line) and DMSO (dashed line)) on ITO to bare ITO. The spectra shown are for an incident angle of 70° and p-polarized IR light. The spectra were obtained from a ratio of 12-phosphonododecanoic acid on ITO to bare ITO. The bare (reference) ITO substrate was cleaned via 20 min of UV/O₃, while the monolayer deposition occurred for 16 h. (Inset: model of 12-phosphonododecanoic acid.)

Table 1. Normal Mode Frequencies of Neat 1-Hexadecanethiol and Frequencies Corresponding to a Monolayer of 1-Hexadecanethiol on ITO and SFO Respectively at an Incidence Angle of 70° with p-Polarized Light

	neat (liquid)	ITO	SFO
$\nu_s\text{CH}_2$ (cm ⁻¹)	2851	2848	2848
$\nu_a\text{CH}_2$ (cm ⁻¹)	2920	2918	2918
$\nu_a\text{CH}_3$ (cm ⁻¹)	2953	2961	2959

Parts A and B of Figure 3 show the reflectance FTIR spectra of an adlayer or partial adlayer of 12-phosphonododecanoic acid on an ITO electrode deposited from either 50/50 (v/v) DMSO/18 MΩ cm H₂O or DMSO at an angle of incidence of 70° for p-polarized light, respectively. The spectra in Figure 3A show vibrational modes corresponding to the symmetric and asymmetric stretching motions of CH₂ groups. As seen in Figure 3B, the carbonyl stretch is observed only for the adlayer formed from 50/50 (v/v) DMSO/18 MΩ cm H₂O deposition solution. Table 2 gives the values of the vibrational frequencies of the adlayer or partial adlayer structures of 12-phosphonododecanoic acid on ITO and the corresponding solid and solution values of these modes.

Table 2. Solid and Solution Values Corresponding to Normal Mode Frequencies of 12-Phosphonododecanoic Acid and the Frequencies of the Corresponding Monolayer or Partial Monolayer of the Same Material on ITO and SFO Respectively at an Incidence Angle of 70° with p-Polarized Light

	solid	solution	ITO ^a	ITO ^b	SFO ^a	SFO ^b
$\nu_s\text{C=O}$ (cm ⁻¹)	1686	1721	1716			
$\nu_s\text{CH}_2$ (cm ⁻¹)	2845	2851	2848	2854	2850	2862
$\nu_a\text{CH}_2$ (cm ⁻¹)	2914	2928	2922	2926	2924	2926

^a 50/50 (v/v) DMSO/18 MΩ cm H₂O. ^b DMSO deposition solution.

The variable angle reflectance FTIR spectra of a partial adlayer of 12-phosphonododecanoic acid on a SFO electrode deposited from either DMSO or 50/50 (v/v) DMSO/18 MΩ cm H₂O show low-intensity modes (below approximately 400 × 10⁻⁶ absorbance units) for a 70° incident angle and p-polarized infrared light (data not shown) in the methylene (CH₂) symmetric and asymmetric stretching region. These modes have a lower intensity and different peak profile as compared to the corresponding modes of an adlayer of 12-phosphonododecanoic acid on ITO. The values of the various vibrational frequencies of

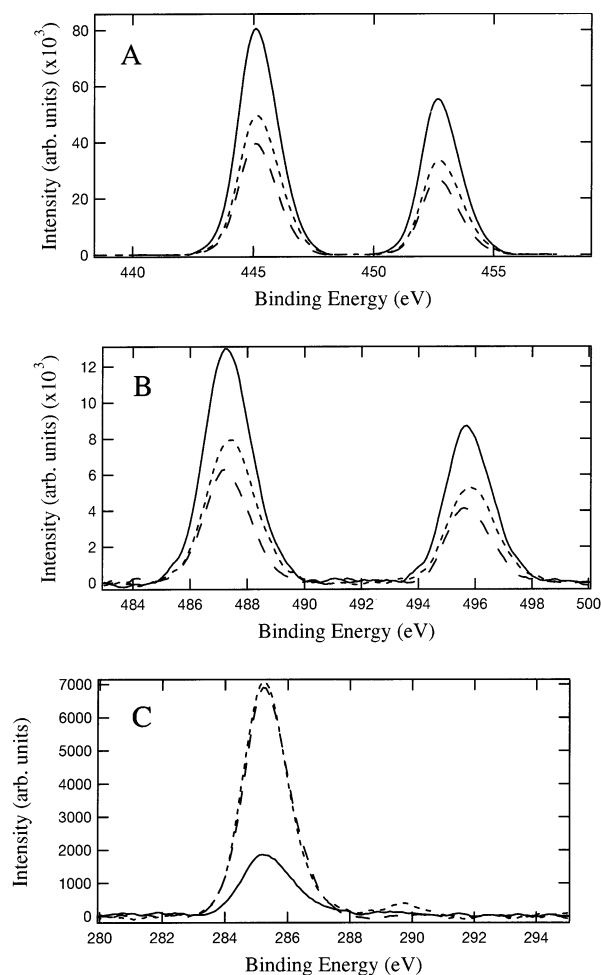


Figure 4. XPS spectra of (A) indium 3d_{5/2,3/2}, (B) tin 3d_{5/2,3/2}, and (C) carbon 1s of bare ITO (solid), 12-phosphonododecanoic acid on ITO (---), and 1-hexadecanethiol on ITO (— · —).

the partial adlayer structures of 12-phosphonododecanoic acid on SFO are listed in Table 2.

The variable angle reflectance FTIR spectra of an ITO surface following application of SDS from 50/50 (v/v) DMSO/18 MΩ cm H₂O show low-intensity peaks (below 3×10^{-4} absorbance units) at 2848 and 2918 cm⁻¹, which correspond to the symmetric and asymmetric CH₂ stretching modes observed at 2849 and 2916 cm⁻¹, respectively, in solid SDS. No observable modes in this region are observed for the deposition of SDS on ITO from 18 MΩ cm H₂O, leading to the conclusion that no adlayer is formed under these conditions. The variable angle FTIR spectra for SDS deposited on SFO electrodes from either 18 MΩ cm H₂O or 50/50 (v/v) DMSO/18 MΩ cm H₂O also do not show any detectable peaks corresponding to SDS on the surface, further substantiating the conclusion that no adlayer is formed by SDS (data not shown).

XPS Characterization. Figure 4A,B shows the XPS spectra of indium 3d_{5/2,3/2} and tin 3d_{5/2,3/2} of bare ITO and an adlayer of either 1-hexadecanethiol or 12-phosphonododecanoic acid (deposited from 50/50 (v/v) DMSO/18 MΩ cm H₂O) on ITO. The positions of the indium 3d_{5/2,3/2} (445.1, 452.7 eV) and tin 3d_{5/2,3/2} (487.2, 495.7 eV) of bare ITO correspond to the In³⁺ and Sn⁴⁺ oxidation states in ITO, respectively.²² These spectra show a significant attenuation of these signals in the spectra corresponding to a monolayer of either 1-hexadecanethiol or 12-phosphonododecanoic acid on ITO relative to bare ITO. Figure 4C shows the carbon 1s spectra of bare ITO, 1-hexadecanethiol on ITO, and 12-phosphonododecanoic

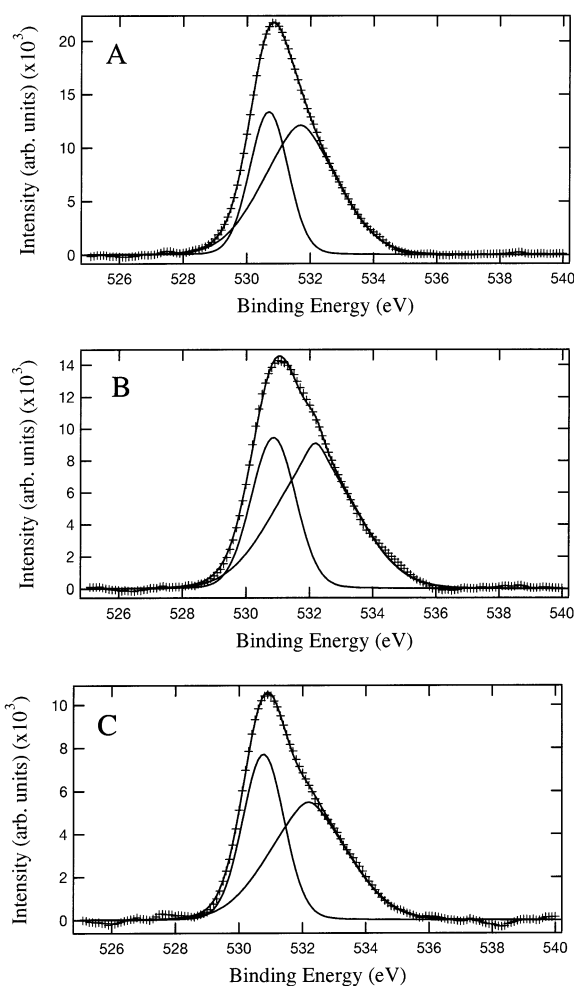


Figure 5. Oxygen 1s XPS spectra of (A) bare ITO (solid), (B) 12-phosphonododecanoic acid on ITO, and (C) 1-hexadecanethiol on ITO. The raw data (markers) and the individual and total 90/10 Gaussian/Lorentzian fits (solid lines) are shown.

acid on ITO. The carbon 1s signal occurs at 285.2 eV (for adventitious carbon on bare ITO), and an increase in this peak is observed for either 1-hexadecanethiol or 12-phosphonododecanoic acid on ITO. An additional peak at 289.7 eV, corresponding to the carbon 1s peak of a carbonyl group, is observed for 12-phosphonododecanoic acid on ITO.²² These results and a summary of the peaks for dodecanethiol, octanethiol, and sodium dodecyl sulfate are in Table 3.

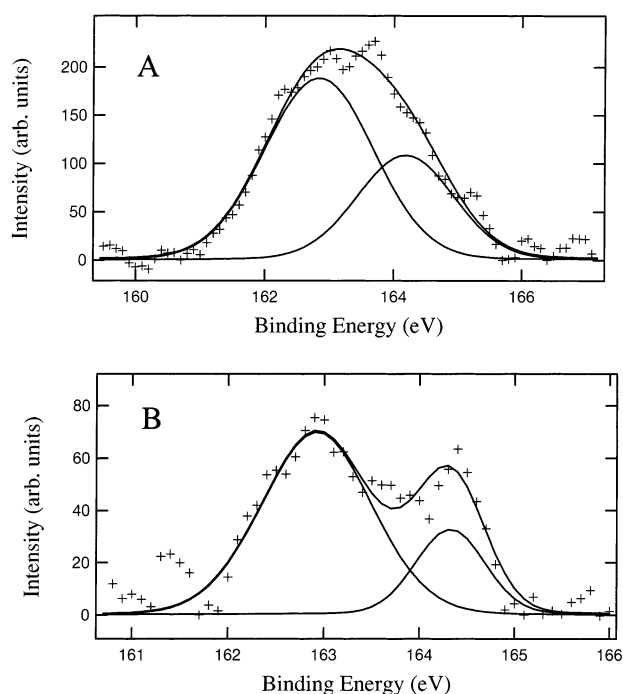
Figure 5 shows the XPS spectra of O 1s of bare ITO, an adlayer of 1-hexadecanethiol on ITO, and an adlayer of 12-phosphonododecanoic acid on ITO. The two components of the O 1s spectra for bare ITO occur at 530.7 and 531.7 eV that correspond to indium oxide and tin oxide species, respectively.²² The ratio between In—O and Sn—O is 1.7 for bare ITO and shifts to 1.6 and 1.3 for 1-hexadecanethiol and 12-phosphonododecanoic acid on ITO, respectively. Also, the peak positions for both of the monolayer structures on ITO are 530.8 and 532.2 eV. The O 1s spectra of the other samples did not show any difference in the peak position or peak area ratio relative to the spectrum of bare ITO.

Figure 6 shows the sulfur 2p_{3/2,1/2} XPS spectra of (A) an adlayer of 1-hexadecanethiol on ITO and (B) a partial adlayer of dodecanethiol on ITO. These peaks occur at 162.8 and 164.2 eV for 1-hexadecanethiol on ITO and at 162.9 and 164.3 eV for dodecanethiol on ITO. There were no observable peaks for octanethiol on ITO (data not

Table 3. In 3d_{5/2,3/2} (445.1, 452.7 eV), Sn 3d_{5/2,3/2} (487.2, 495.7 eV), and C 1s (285.2 eV) XPS Intensities and Percentage Differences from Bare ITO Reference

	In 3d _{3/2}	In 3d _{5/2}	Sn 3d _{3/2}	Sn 3d _{5/2}	C 1s
bare ITO	55300	80664	8709	12994	1860
1-hexadecanethiol	26737	39577	4133	6287	6895
	(−52%)	(−51%)	(−53%)	(−52%)	(+271%)
dodecanethiol	40729	58617	6393	9118	3966
	(−26%)	(−27%)	(−27%)	(−30%)	(+113%)
octanethiol	44859	64854	7535	10736	2532
	(−19%)	(−20%)	(−13%)	(−17%)	(+36%)
12-phosphonododecanoic acid ^a	33417	49442	5297	7930	7068
	(−40%)	(−39%)	(−39%)	(−39%)	(+280%)
12-phosphonododecanoic acid ^b	44573	65276	6478	9969	4537
	(−19%)	(−19%)	(−26%)	(−23%)	(+144%)
sodium dodecyl sulfate ^c	49141	72095	7514	11554	2572
	(−11%)	(−11%)	(−14%)	(−11%)	(+38%)

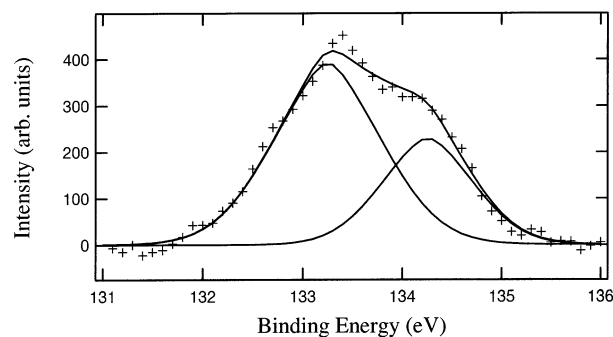
^a 50/50 (v/v) DMSO/18 MΩ cm H₂O. ^b DMSO. ^c 18 MΩ cm H₂O deposition solvent system.

**Figure 6.** Sulfur 2p_{3/2,1/2} XPS spectra corresponding to (A) an adlayer of 1-hexadecanethiol on ITO and (B) a partial adlayer of dodecanethiol on ITO. The raw data (markers) and the individual and total 90/10 Gaussian/Lorentzian fits (solid lines) are shown.

shown). The overall peak intensities for dodecanethiol and octanethiol on ITO are 90 and 0% of the intensity of sulfur 2p_{3/2,1/2} relative to 1-hexadecanethiol on ITO, respectively. The peak positions for 1-hexadecanethiol and dodecanethiol are characteristic of a thiolate species of the alkane thiols.^{2,22}

Figure 7 shows the phosphorus 2p_{3/2,1/2} signals at 133.2 and 134.3 eV, respectively, from an adlayer of 12-phosphonododecanoic acid (deposited from 50/50 (v/v) DMSO/18 MΩ cm H₂O) on ITO. These peak positions correspond to a fully deprotonated phosphonate group (PO₃^{2−}).^{26–28} The corresponding phosphorus 2p_{3/2,1/2} peak intensities are 30% lower for the partial adlayer formed from DMSO (data not shown).

Modeling of the 12-Phosphonododecanoic Acid Monolayer. Figure 8 shows the infrared spectra of two possible forms of the carboxylic acid functional group of

**Figure 7.** Phosphorus 2p_{3/2,1/2} (133.2, 134.3 eV) XPS spectra of 12-phosphonododecanoic acid on ITO. The raw data (markers) and the individual and total 90/10 Gaussian/Lorentzian fits (solid lines) are shown.

12-phosphonododecanoic acid calculated using DFT methods. Figure 8 shows the calculated frequency spectra for the acid (COOH) form of this molecule with a carbonyl stretch at 1772 cm^{−1}, while the highest stretching frequency of the carboxylate (COO[−]) group is at 1523 cm^{−1}. The frequency decrease in the carboxylate species is the result of a decrease in bond order between the carbon and oxygen atoms.

Modeling of Frequency Shifts upon Adlayer Formation. The experimental observation of a lowering of the vibration frequency of methylene CH₂ stretches upon adlayer formation as compared to solution values was successfully modeled theoretically using periodic boundary conditions (PBC). The model was polymethylene with 12 methylene groups in each subunit. The model is similar to an infinite chain of methylene groups because the distance between carbon atoms in adjacent subunits (boxes) is the same as the distance between carbon atoms in the same subunit. The box length perpendicular to the molecular axis of the molecule was varied to simulate the effect of close packing in adlayers. Figure 9 shows the calculated frequency spectra for two different box dimensions. The mode type and the corresponding frequencies are listed in Table 4. As seen in Figure 4, as the box dimension becomes smaller the symmetric and asymmetric methylene CH₂ stretches decrease compared to the corresponding frequencies with a larger box dimension. This effect is similar to the experimental result that occurs upon adlayer formation due to the molecules coming into closer contact as compared to in solution. Similar trends were found using PBC with both 12-phosphonododecanoic acid and 1-hexadecanethiol.

Enthalpic Considerations in Monolayer Formation. The enthalpic contribution to monolayer formation was modeled using density functional calculations with

(26) Kohli, P.; Blanchard, G. *Langmuir* **2000**, *16*, 8518–8524.

(27) Petruska, M.; Fanucci, G.; Talham, D. *Chem. Mater.* **1998**, *10*, 177–189.

(28) Seip, C.; Talham, D. *Mater. Res. Bull.* **1999**, *34*, 437–445.

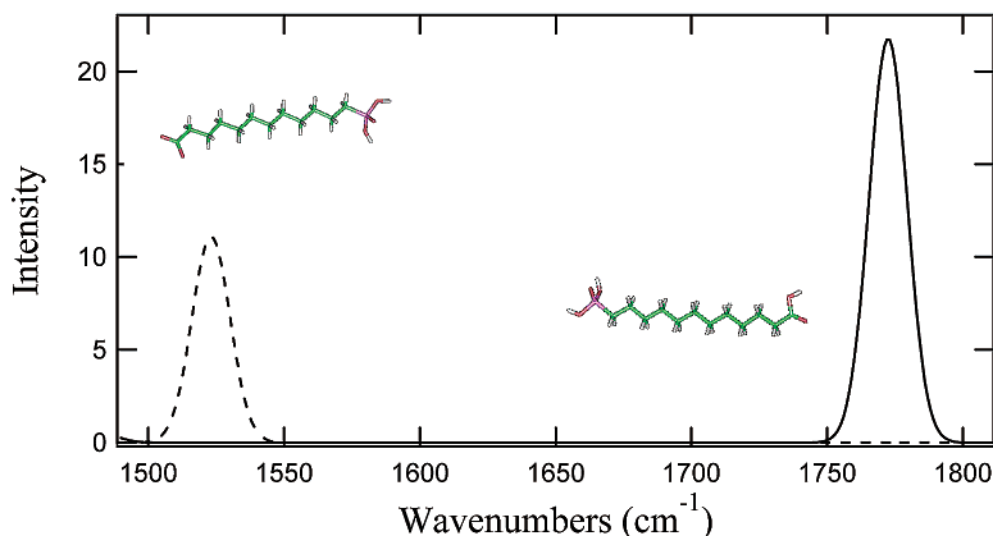


Figure 8. DFT calculated frequency spectra of the carboxylic acid (solid line) and carboxylate (dashed line) forms of 12-phosphonododecanoic acid. The spectra have a Gaussian width of 7 cm^{-1} . (Insets: models corresponding to the two spectra.)

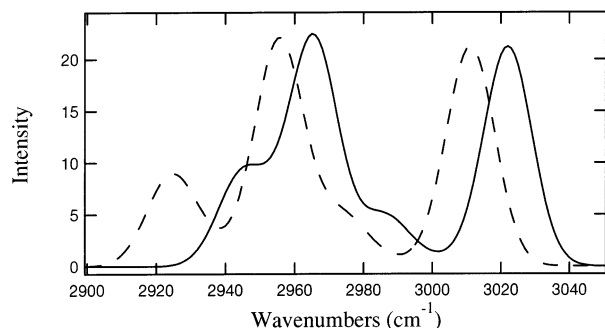


Figure 9. Calculated frequency spectra for polymethylene (12 methylene groups per box) using PBC for different box dimensions. The box dimensions are defined by sides a , b , and c . The molecular axis of the molecule is parallel to the a direction. The box angles are 60° , while the lengths for a , b , and c are 15, 10, and 10 Å (solid curve) and 15, 10, and 6 Å (dashed curve), respectively. The length of the box along the a direction makes the distance between carbon atoms in adjacent boxes to be the same as between carbon atoms along the alkane chain in the same box. The spectra have a Gaussian width of 7 cm^{-1} .

Table 4. Calculated Frequencies for Polymethylene (12 Methylene Groups per Box) Using PBC with Two Different Box Dimensions^a

	$\text{C}_{12}\text{H}_{24}^b$	$\text{C}_{12}\text{H}_{24}^c$	difference
$\nu_s\text{CH}_2\text{ (cm}^{-1}\text{)}$	2946	2925	21
$\nu_s\text{CH}_2\text{ (cm}^{-1}\text{)}$	2965	2956	9
$\nu_a\text{CH}_2\text{ (cm}^{-1}\text{)}$	2987	2976	11
$\nu_a\text{CH}_2\text{ (cm}^{-1}\text{)}$	3022	3011	11

^a The box angles were 60° . (Length a is parallel to the molecular axis of the molecule while b and c are perpendicular to a). ^b Box dimensions: 15, 10, and 10 Å for a , b , and c , respectively. ^c Box dimensions: 15, 10, and 6 Å for a , b , and c , respectively.

PBC. The energetics of headgroups of adlayer molecules interacting with atoms of the surface can be quantified by calculating potential energy surfaces (PES) corresponding to these interactions in the gas phase. PBC models can be used to model the dispersion forces between adjacent alkane chains. PBC calculations use arrays, with subunits of defined dimensions, each containing one molecule. Therefore, by changing the dimensions of the subunits one can study the energetics between adjacent molecules (subunits). Potential energy surfaces for the binding of sulfur (of 1-hexadecanethiol) to either indium or tin (with

hydroxyl groups completing the coordination shell of the metal) are shown in Figure 10A. These curves show a binding energy of -118 and -155 kJ/mol for the S–Sn (2.55 Å) and S–In (2.45 Å) bonds, respectively. Similar PES of the binding of the deprotonated phosphonate (PO_3^{2-}) form of 12-phosphonododecanoic acid to either tin or indium (with hydroxyl groups completing the coordination shell of the metal) showed binding energies of -98 (2.97 Å) and -116 (2.82 Å) kJ/mol , respectively (data not shown). Figure 10B shows the PES of varying the box width (perpendicular to the molecular axis of the molecule) of 1-hexadecanethiol and 12-phosphonododecanoic acid to illustrate the enthalpic contribution to monolayer formation from interaction between neighboring molecules. These potential energy surfaces show an enthalpy of interaction of -34 and -22 kJ/mol for 1-hexadecanethiol and 12-phosphonododecanoic acid, respectively. Similar calculations for dodecanethiol and octanethiol showed an enthalpy of interaction of -19 and -3 kJ/mol , respectively, as shown in Figure 10C. The absolute value of this enthalpy of interaction is likely greater for 1-hexadecanethiol primarily due to the larger number of methylene groups that can interact with neighboring alkane chains, as shown with the alkane thiols of varied alkane chain length, and due to the bulky functional groups of 12-phosphonododecanoic acid limiting the distance between neighboring alkane chains. The expected correlation that the enthalpy of interaction of adjacent alkane chains decreases as the alkane chain length decreases was shown with alkane thiols of varied chain length. Although the trends are correct, the calculated dispersion forces are smaller than those that are experimentally measured.²¹ As calculated, these dispersion forces are considerably smaller (ca. -10 to -30 kJ/mol) than the binding energy of either the thiolate or phosphonate group to In or Sn (ca. -100 to -150 kJ/mol). Closer packing of the chains could lead to nearly comparable values for these two enthalpies.

Sequential Electrode Immersions. The stabilities of the adlayer structures of 1-hexadecanethiol and 12-phosphonododecanoic acid on ITO were investigated through exchange reactions. The ITO electrodes that were first immersed in 10 mM 12-phosphonododecanoic acid in 50/50 (v/v) DMSO/18 MΩ cm H_2O (16 h) were then immersed in 1-hexadecanethiol (16 h) and vice versa. The resulting reflectance FTIR spectra showed that neither of

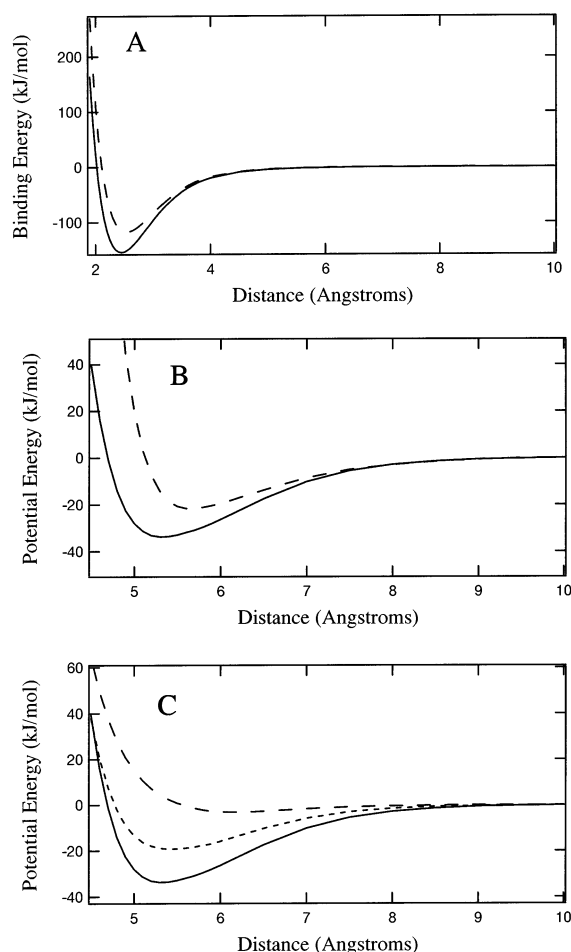


Figure 10. (A) PES of the binding of S (of 1-hexadecanethiol) to In (solid line) or Sn (dashed line) in the gas phase. (B) PES of varying the width of the box (subunit) using periodic boundary conditions for 1-hexadecanethiol (solid line) and 12-phosphonododecanoic acid (dashed line) with box angles of 60° . The length along the molecular axis of the molecules was 30 Å and one length perpendicular to the molecular axis was 10 Å, while the final length (perpendicular to the molecular axis) was varied from 4.5 to 10 Å to obtain the PES. (C) PES of varying the width of the box using periodic boundary conditions for 1-hexadecanethiol (solid line), dodecanethiol (---), and octanethiol (- -) using the same protocol as for 1-hexadecanethiol in (B). The potential energies were referenced to 10 Å for (A), (B), and (C).

the adlayers were displaced by the other molecule (data not shown). Earlier work showed that phosphonic acids have a higher affinity than thiols to form adlayers on ITO,¹⁵ which is similar to the present results where an adlayer of 1-hexadecanethiol on ITO was formed only when deposited from the corresponding neat thiol while 12-phosphonododecanoic acid formed an adlayer on ITO from a much more dilute deposition solution (10 mM) of the phosphonic acid.

Discussion

FTIR reflectance measurements have shown that indium–tin oxide (and SFO) electrodes are highly reflective in the mid-IR region ($650\text{--}4000\text{ cm}^{-1}$) and that the reflectance is a function of incident angle, polarization, and wavenumber.²⁵ This high reflectivity allows reflectance FTIR spectroscopy to probe structures on the surfaces of these two electrodes. The combination of reflectance FTIR spectroscopy and X-ray photoelectron spectroscopy provides evidence that chemisorbed adlayers

of alkanethiols and phosphonates form on ITO and SFO films.

Reflectance FTIR and XPS show that a close-packed, stable monolayer structure of 1-hexadecanethiol is formed on ITO and SFO electrodes through a thiolate interaction with the metal atoms of the surface. Our XPS results agree with those of a previous report,²² and the optical spectroscopy lends further support to the hypothesis that the thiolate film is well-ordered. Variable angle reflectance FTIR spectroscopy demonstrates an ordered monolayer structure on both ITO and SFO electrodes by the decrease of the frequency of the CH_2 methylene stretches relative to those of neat 1-hexadecanethiol and by their signal intensities. This frequency decrease is the result of packing interactions between neighboring molecules as the close-packed monolayer is formed, which was successfully modeled using periodic boundary conditions. The position of the sulfur $2p_{3/2,1/2}$ signal, the attenuation of indium $3d_{5/2,3/2}$ and tin $3d_{5/2,3/2}$, and the increase in carbon $1s$ XPS signals relative to those of bare ITO demonstrates the presence of a monolayer of 1-hexadecanethiol on ITO with a thiolate–metal interaction;^{2,22} however, the preferential affinity of the thiolate–metal interaction for either indium or tin cannot be deduced from the experimental data.²²

The formation of a monolayer of 1-hexadecanethiol on either ITO or SFO is enthalpically driven by the thiolate–metal (In or Sn) interaction and the interaction between neighboring alkane chains. The DFT PES calculations show that the S–In is more energetically stable than the S–Sn interaction. Although the majority of the enthalpic driving force is from the thiolate–metal interaction, there is some enthalpic gain from the packing interactions. The enthalpy of interaction of alkane chains was found to decrease as the chain length decreased, similar to previous experimental work;²¹ however, the absolute value of the calculated enthalpy of interaction will depend on the periodic boundary conditions used. This enthalpic difference contributes to the formation of complete adlayers as the chain length is increased. As observed previously on Au surfaces,^{3,21} the chain length dependence of film stability is demonstrated experimentally here by the formation of a partial monolayer of dodecanethiol and the lack of any monolayer structure of octanethiol. Evidence for the relative coverage as a function of alkane chain length is found in the relative attenuation of the indium $3d_{5/2,3/2}$ and tin $3d_{5/2,3/2}$ XPS signals and the small or absent sulfur $2p_{3/2,1/2}$ signal for dodecanethiol or octanethiol, respectively. However, given that the In–S bond is stronger than the dispersion forces between adjacent alkane chains, entropic effects (not modeled here) must contribute significantly to the energetics of adlayer formation. The competing entropic factors for the alkane thiols are sequestering in solvent analogous to micelle formation versus forming an adlayer due to the hydrophobic effect.

12-Phosphonododecanoic acid also formed a close-packed, stable monolayer structure on ITO as shown by reflectance FTIR and XPS through the interaction between fully deprotonated phosphonate groups (PO_3^{2-}) and metal atoms of the surface when deposited from 50/50 (v/v) DMSO/18 MΩ cm H_2O . The position of the XPS phosphorus $2p_{3/2,1/2}$ peak shows that the phosphonate group is in the PO_3^{2-} form in this monolayer structure and that only a partial monolayer is formed from DMSO by the relatively smaller attenuation of the indium $3d_{5/2,3/2}$ and tin $3d_{5/2,3/2}$ XPS signals and a decrease in the carbon $1s$ and phosphorus $2p_{3/2,1/2}$ signals,^{26–28} therefore demonstrating that monolayer formation of 12-phosphonododecanoic acid is highly dependent upon the deposition parameters.

Reflectance FTIR spectroscopy demonstrated a close-packed, ordered monolayer structure of 12-phosphonododecanoic acid when deposited from 50/50 (v/v) DMSO/18 MΩ cm H₂O from the signal intensities and from the frequencies of the carbonyl and methylene CH₂ stretches being intermediate between the solid and solution values of these frequencies. The decrease in frequencies of these vibrations as compared to solution values is again the result of packing interactions between neighboring chains in the monolayer. However, the increase in the methylene CH₂ symmetric stretch relative to the solution values demonstrates that a disordered structure was formed when 12-phosphonododecanoic acid was deposited from DMSO on ITO.

The enthalpic driving forces for the formation of a monolayer of 12-phosphonododecanoic acid on ITO are the interaction between the phosphonate group and the metal atoms of the surface and the packing interactions. DFT calculations showed that the phosphonate–indium interaction is thermodynamically more stable than the corresponding phosphonate–tin interaction. Also, the binding energy for phosphonate is smaller than the corresponding thiolate (of 1-hexadecanethiol) interaction with either metal atom. Therefore, along with the smaller packing stabilization energy as compared to that of 1-hexadecanethiol, the monolayer of 12-phosphonododecanoic acid forms a theoretically enthalpically less stable monolayer than 1-hexadecanethiol. However, neither molecule could replace an existing monolayer structure of the other molecule on ITO. Moreover, the carboxylic acid of 12-phosphonododecanoic is protonated in the monolayer structure formed from 50/50 (v/v) DMSO/18 MΩ cm H₂O based on DFT frequency calculations of the carbonyl or carboxylate forms and literature values of carboxylate stretching frequencies of carboxylate groups interacting with oxidized aluminum surfaces.¹² For example, *n*-alkanoic acids interacting with oxidized aluminum surfaces in the carboxylate form experimentally showed a frequency at 1608 cm⁻¹ on metal oxide surfaces

involving carbon and oxygen.¹² The lack of a carbonyl frequency in the DMSO-deposited material suggests that the transition dipole moment of the carbonyl group is parallel to the surface.

Many of the conditions used did not lead to formation of ordered monolayers on the two metal oxides studied. On the basis of the reflectance FTIR and XPS data signal intensities, no monolayers were formed by sodium dodecyl sulfate on ITO or SFO electrodes or by 12-phosphonododecanoic acid on SFO by any of the deposition solvent systems used. All of these samples showed no or low-intensity signals in the reflectance FTIR spectra and little if any attenuation of indium 3d_{5/2,3/2} and tin 3d_{5/2,3/2} or an increase in carbon 1s XPS signals (or presence of other elements of the monolayer material).

Conclusion

Variable angle reflectance FTIR spectroscopy was shown to be effective in characterizing adlayers on both ITO and SFO electrodes due to their high reflectivity in the mid-IR. Reflectance FTIR and XPS showed that an adlayer of 1-hexadecanethiol formed on both ITO and SFO through a thiolate–metal interaction while an adlayer of 12-phosphonododecanoic acid was observed on ITO through a phosphonate–indium interaction. The enthalpic factors contributing to adlayer formation were found to be packing interactions between neighboring alkane chains and the interaction of thiolate or phosphonate groups with the metal atoms of the surface. The importance of these packing interactions was shown by a decrease in both the DFT calculated enthalpy of interaction of neighboring alkane chains and the relative surface coverage on ITO of alkane thiols as the alkane chain length decreased.

Acknowledgment. Scott Brewer was supported by NIH Biotechnology Training Grant T32-GM08776. Support and computational facilities were provided by the North Carolina Supercomputing Center.

LA015720D